Chinese Chemical Letters 34 (2023) 107557

Contents lists available at ScienceDirect

Chinese Chemical Letters

journal homepage: www.elsevier.com/locate/cclet

A novel TICT-based near-infrared fluorescent probe for light-up sensing and imaging of human serum albumin in real samples

Yufan Fan[a,1], Fangyuan Wang[a,d,1], Fanbin Hou[a], Lai Wei[b], Guanghao Zhu[a], Dongfang Zhao[a], Qing Hu[a], Tao Lei[c], Ling Yang[a,*], Ping Wang[a,*], Guangbo Ge[a,*]

[a] Shanghai Frontiers Science Center of TCM Chemical Biology, Institute of Interdisciplinary Integrative Medicine Research, Shanghai University of Traditional Chinese Medicine, Shanghai 201203, China
[b] Key Lab of Separation Science for Analytical Chemistry, Dalian Institute of Chemical Physics, Chinese Academy of Sciences, Dalian 116023, China
[c] Putuo Hospital, Shanghai University of Traditional Chinese Medicine, Shanghai 200062, China
[d] Key Laboratory of Liver and Kidney Diseases (Ministry of Education), Institute of Liver Diseases, Shuguang Hospital, Shanghai University of Traditional Chinese Medicine, Shanghai 201204, China

ARTICLE INFO

Article history:
Received 11 March 2022
Revised 9 May 2022
Accepted 23 May 2022
Available online 27 May 2022

Keywords:
Human serum albumin
Near-infrared probe
High-throughput detection
Confocal imaging

ABSTRACT

Human serum albumin (HSA) has emerged as a pivotal biomarker and prognostic indicator for various human diseases. Real-time sensing and visual tracking of HSA in plasma or other biological systems will immensely facilitate the basic researchers and clinicians to better understand HSA-associated biological processes. Herein, a novel near-infrared (NIR) fluorescent probe (**7-HTCF**) was rationally constructed for light-up sensing and *in-situ* imaging of HSA in real samples, based on the principle of twisted intramolecular charge transfer (TICT). Under physiological conditions, **7-HTCF** could be efficiently trapped by HSA to form a stable complex *via* binding on a non-drug binding site, while the complex emitted strong fluoresce signals around 670 nm. Further investigations demonstrated that **7-HTCF** displayed a great combination of excellent selectivity and good chemical stability, as well as rapid fluorescent response and ultra-high sensitivity for HSA detection. Particularly, the newly developed light-up probe has been successfully utilized for quantitative detection of HSA in diluted plasma samples, while its readouts are hardly affected by the addition of therapeutic agents and herbal medicines. **7-HTCF** is also successfully used for *in-situ* imaging of the reabsorbed HSA in living renal cells, while this dye exhibits good cell permeability and high resolution for *in-situ* imaging in living cells. Collectively, a novel TICT-based near-infrared fluorescent probe was devised for highly selective and ultra-sensitive sensing of HSA in plasma samples or imaging HSA in living cells, which offered a practical tool for clinical tests and for exploring HSA-associated biological processes.

Human serum albumin (HSA) is the most abundant protein in serum, accounting for up to 50% of circulating proteins in healthy individuals [1,2]. Following synthesized in hepatocytes, HSA will be readily secreted into the portal circulation without any modifications, with a half-life of 19–21 days [3,4]. HSA plays pivotal roles in regulating the colloid osmotic pressure and acts as a versatile carrier for a wide range of endogenous substances and xenobiotics [1,5]. Furthermore, HSA also has numerous other functions, such as anti-oxidative, immunomodulatory, and neuroprotective activity [4,6]. As a valuable biomarker, the abnormal level of albumin in blood or urine can reflect diverse pathological conditions, including sepsis, hepatopathy (hepatitis or liver cirrhosis), nephropathy (glomerular or tubules injury) and systemic inflammatory [7–9]. Moreover, HSA is widely used to treat several diseases in clinical, such as hypovolemia, burns, surgical blood loss, hemodialysis, acute liver failure [4]. Therefore, the practical tools for rapidly and reliably detecting endogenous HSA are always desirable.

Over the past decades, several techniques including dye-binding methods, immunochemical assays, and biomass spectrometry-based techniques, have been applied for quantifying HSA [10–12]. Among these assays, fluorescent dyes have aroused great attention, owing to their inherent advantages including high sensitivity, easy to use, capable for high-throughput detection and *in-situ* visualization or dynamic tracking of HSA (Table S1 in Supporting information) [13,14]. Currently, two major classes of HSA fluorescent

* Corresponding authors.
E-mail addresses: yling@shutcm.edu.cn (L. Yang), pwang@shutcm.edu.cn (P. Wang), geguangbo@shutcm.edu.cn (G. Ge).
[1] These authors contributed equally to this work.

https://doi.org/10.1016/j.cclet.2022.05.071
1001-8417/

probes including enzyme-activatable fluorescent substrates (based on the *pseudo*-esterase activity of HSA) and dye-binding fluorescent probes (mainly based on the hydrophobic binding property of HSA), have been reported [10,15,16]. The enzyme-activatable HSA substrates displayed poor sensitivity even after long incubation time, while the fluorescence signals of dye-binding HSA probes could be easily affected by either endogenous substances or xenobiotics (such as drugs, herbal/food chemicals) [17]. For instance, the detection of bromocresol green (BCG) and bromocresol purple (BCP) could be interfered by uremic toxins, as well as other agents that bind on HSA at drug-binding sites IIA and IIIA [18,19]. Additionally, most reported dye-binding probes are restricted in short emission wavelengths or high background signal [20]. Near-infrared (NIR) probes can efficiently offset these shortcomings because of the improved signal-to-noise ratio and higher imaging resolution [21–23]. Therefore, there is an urgent need for designing and developing more practical NIR fluorescent probes with high selectivity, improved optical features and excellent sensitivity for sensing and imaging HSA in real samples.

Herein, on the basis of 3D structure of HSA and its excellent ligand-binding capacity towards small hydrophobic molecules, a panel of TICT fluorescent dyes (Table S2 in Supporting information) with a donor-π-acceptor (D-π-A) structure are rationally designed [17,24,25]. Coumarin is selected as a basic fluorophore (electron donor), owing to its inherent advantages including the controllable emission spectrum, significant Stokes shift, low toxicity, and good cell membrane permeability [26,27]. A π-conjunction unit, which is responsible for connecting various acceptors to coumarin, enables the sensor to have unconstrained intramolecular rotation [17,28]. Mechanistically, the donor and acceptor fragment are gradually twisted into a perpendicular conformation, resulting in the complete charge separation and facilitating a high TICT formation rate [28]. Usually, the TICT fluorophore is non-emissive when it is in the TICT state (unbound and free rotating state). By contrast, once the TICT-type fluorescent dye is bound on the hydrophobic pocket of HSA, the twist of D/A pair will be strongly restricted, which in turn, bring a strong fluorescence signal [29,30]. Subsequently, these TICT-type probes were virtually screened by molecular docking simulations, with affinity score and binding mode as criteria. Probe **1** (((*E*)−2-(3-cyano-4-(2-(7-hydroxy-2-oxo-2*H*-chromen-3-yl)vinyl)-5,5-dimethylfuran-2(5*H*)-ylidene)malononitrile), **7-HTCF**) exhibited the strongest binding affinity, whose conformation distribution and binding modes stably gathered in domain IA&B, differ from the classical drug-binding sites (IIA and IIIA). Structurally, the acceptor moiety of 7-HTCF, TCF (2-dicyanomethylene-3-cyano-4,5,5-trimethyl-2,5-dihydrofuran), is well suited as an electron acceptor to further tune the push-pull effect and intramolecular charge transfer (ICT) characteristics, due to its superiorities of the strong electron-withdrawing property, long emission wavelength, and good binding-affinity towards albumin cavities [31–33]. Therefore, the optimized probe was synthesized, characterized, and used for further investigations (Scheme S1, Figs. S1–S4 in Supporting information).

Rejoicingly, **7-HTCF** exhibited exceptional sensing ability towards HSA (Scheme 1). Upon the addition of HSA, the absorption peak of the probe showed to a significant red-shift from 570 nm to 630 nm, accompanied by a distinct color change (Fig. 1). Such color change from purple to blue indicated that **7-HTCF** could serve as a "naked-eye" colorimetric indicator for HSA. Meanwhile, **7-HTCF**-HSA complex elicited an over 68.5-fold enhancement in fluorescence intensity around 670 nm (upon excitation at 630 nm). The fluorescence quantum yields of the probe and its complex were 0.009 and 0.189, respectively (Table S3 in Supporting information). This mechanism, we envisaged, may be due to the hydrophobic cavity that limits the innate intramolecular rotation, thereby

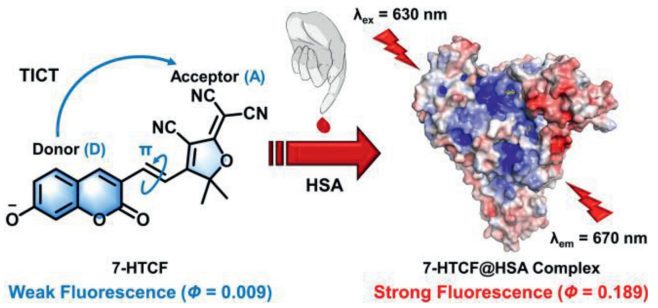

Scheme 1. The structure of **7-HTCF** and proposed sensing mechanism towards HSA.

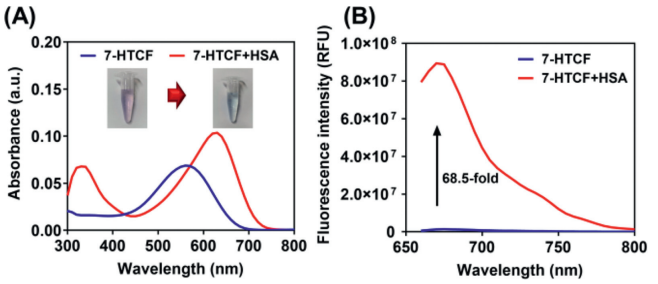

Fig. 1. The changes in absorption (A) and fluorescence spectra (B) of **7-HTCF** (10 μmol/L) in the presence or absence of HSA (10 μmol/L).

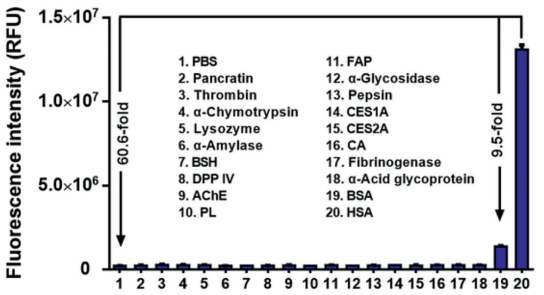

Fig. 2. The fluorescence intensity of **7-HTCF** (10 μmol/L) in the presence of HSA or other tested human plasma protein under physiological conditions (pH 7.4 at 37 °C) for 5 min.

increasing the molecular coplanarity and facilitating the valence electron transition [17]. Then, the hypothesis that restricting intramolecular rotation can trigger a prominent effect was verified by a viscosity-dependent fluorescence (Fig. S5 in Supporting information) [29,34]. Briefly, HSA can dramatically improve and stabilize the optical properties of **7-HTCF** by restricting D/A twist and immobilizing conformation [31]. The solvent effects of the probe are consistent with a previous report that the TICT state will be significantly stabilized in polar solvents (Fig. S6 in Supporting information) [28]. Furthermore, **7-HTCF** could rapidly bind HSA to form a stable complex with excellent photostability and thermal stability (Figs. S7A–C in Supporting information). The complex was extraordinarily susceptible from pH 7.0 to 9.0 while attaining the maximum at pH 8.0 (Fig. S7D in Supporting information). It is expected to sense HSA in complex biological samples stably.

Subsequently, the specificity and anti-interference ability were further investigated. Only HSA triggered a conspicuous fluorescence enhancement, while other human serum proteins, including AAG, another high-abundance serum protein, exerted negligible changes (Fig. 2). Although BSA shared high homology and similar structure with HSA, the fluorescence intensity of the **7-HTCF**-HSA complex was 9.5-fold higher over that of BSA. Moreover, a diverse array of endogenous compounds, commonly therapeutic drugs, natural products, and traditional Chinese medicine injection,

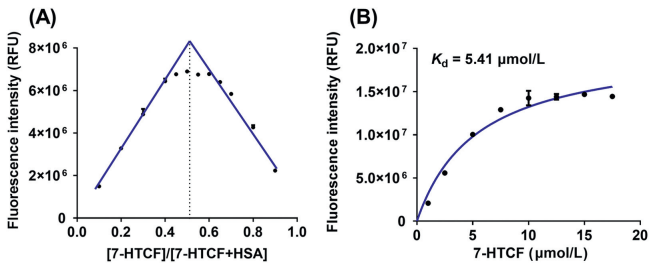

Fig. 3. (A) Job's plot analysis of fluorescence at 670 nm against [**7-HTCF**]/([**7-HTCF**] + [HSA]), while the total concentration was set at a constant value of 10 μmol/L. (B) The binding affinity and kinetic analysis of **7-HTCF** on HSA.

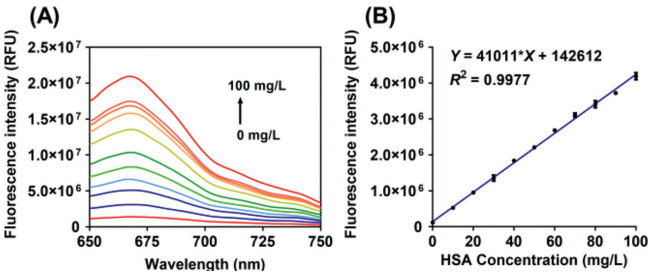

Fig. 4. (A) Fluorescence spectra of **7-HTCF** (20 μmol/L) co-incubated with increasing concentrations of HSA (0–100 mg/L) in PBS. (B) The quantitative curve of HSA in PBS.

also barely intervened in the detection (Figs. S8 and S9, Table S4 in Supporting information). The newly light-up probe performed powerful anti-interference and superior specificity towards HSA over other human proteins and biological analytes. Under physiological conditions, **7-HTCF** holds excellent potential for reliable and specific detection.

The binding properties were also characterized to elucidate its response mechanism. Fluorescence quenching assays showed that the intrinsic fluorescence of HSA can be significantly inhibited upon addition of the increasing concentrations of **7-HTCF** (Fig. S10 in Supporting information). The calculated K_{sv} and K_q values were 1.65×10^4 L/mol and 1.65×10^{12} L mol^{-1} s^{-1}, respectively, in which the K_q value was much greater than the maximum scatter collision quenching constant (2.0×10^{10} L mol^{-1} s^{-1}). These findings suggest that the quenching process of HSA by **7-HTCF** is a classic static mechanism, suggesting that the probe can tightly bind in HSA to form a stable complex [35]. By constructing the fluorescence intensity at 670 nm as a function of **7-HTCF** molar fraction, Job's plot analysis was depicted to determine binding stoichiometry. Fluorescence attained the maximum as the molar fraction of **7-HTCF** reached about 1/2 (Fig. 3A), indicating that the formation of probe-HSA complex followed a 1:1 stoichiometry. Then, the binding affinity and kinetic analysis further revealed that **7-HTCF** had a relatively high affinity for HSA, with an apparent dissociation constant (K_d) of 5.41 μmol/L (Fig. 3B). Drug replacement assay further identified the specific binding site. A series of marker drugs were selected, including paclitaxel (subdomain IA), ibuprofen (subdomain IIA), diflunisal (subdomain IIA), warfarin (a site marker of subdomain IIA), propofol (subdomains IIIA and IIIB), digoxin (subdomain IIIA), and salicylic acid (subdomains IIA and IB) [36,37]. Strangely, these site-specific drugs scarcely affected the fluorescence of the complex, even at high concentrations (Fig. S11 in Supporting information). In brief, **7-HTCF** could bind tightly to HSA through a non-drug binding site to form a stable complex with extremely anti-interference ability, which may be one cause for its readouts were barely affected by the addition of therapeutic agents and herbal medicines.

Next, a fluorescence titration analyzed the linear response of **7-HTCF** towards HSA quantitatively. The calibration curve revealed a satisfactory correlation ($R^2 = 0.9977$) over the range of 1–100 mg/L (Fig. 4). The detection limit (LOD) was as low as 1.32 mg/L, which was more than enough for quantifying HSA in clinical. Furthermore, considering the influence of the biological matrix, the calibrate curve was established in diluted plasma samples before quantitative applications (Fig. S12 in Supporting information). The recovery and precision of the method were fully investigated (Table S5 in Supporting information). Later, **7-HTCF** was employed as a rapid-response tool to quantify HSA levels in 20 healthy volunteers, while the BCG method served as a control method (Table S6 in Supporting information). Human plasma samples and ethical approval was originated from Putuo Hospital, Shanghai Uni-

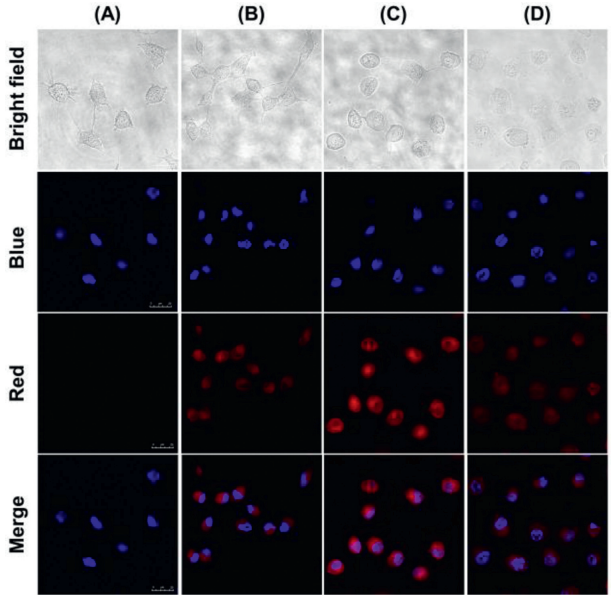

Fig. 5. *In-situ* fluorescence imaging of HSA reabsorption in RPTEC cells using **7-HTCF**. (A-C) Cells were treated with **7-HTCF** (10 μmol/L) for 30 min and followed by addition of 0, 0.5 and 1 mg/mL HSA, respectively. (D) Cells were co-incubated with probe for 30 min, then HSA (1 mg/mL) and rifampicin were added.

versity of Traditional Chinese Medicine (Shanghai, China). Everyone participating in this project has signed the informed consent. The HSA level determined by the **7-HTCF** method agreed well with the BCG method, with a difference of less than 10%. Its readouts are hardly affected by the addition of herbal medicines. Moreover, **7-HTCF**-based assays just required a 1000-fold dilution of plasma, which meant that 1 μL plasma could be sufficient for HSA quantification. Above all, **7-HTCF** can reliably and stably detect HSA in human plasma, providing a promising tool for the clinical diagnosis of HSA-associated diseases.

In healthy individuals, normal urinary albumin levels mainly rely on the limited glomerulus filtration and the proximal tubules reabsorption [38]. RPTEC cell was used as the renal cell model to visualize the albumin reabsorption. Before the imaging, a standard CCK-8 assay indicated that **7-HTCF** was applicable for the envisaged intracellular albumin imaging with good biocompatibility (Fig. S13 in Supporting information). Following co-incubation with **7-HTCF** for 30 min (Fig. 5A), no distinct red fluorescence in RPTEC cells (without HSA), suggesting that the probe had certain stability in the incubation system. In sharp contrast, the intensive fluorescence appeared upon addition with HSA, positively correlated with HSA concentration (Figs. 5B and C). Beside, rifampicin (a nephrotoxic drug) significantly diminished fluorescence (Fig. 5D). It is re-

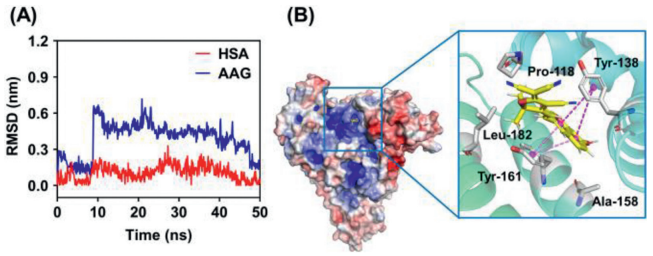

Fig. 6. (A) Root mean square deviation (RMSD) analysis of **7-HTCF** bound on the subdomain IB of HSA and AAG. (B) The binding pose of **7-HTCF** (yellow) on HSA in panorama and part.

ported that rifampicin often induces adverse renal effects, from mild proteinuria to acute renal failure; it may impair the renal uptake capacity [39,40]. **7-HTCF** could serve as a reliable bioimaging tool for albumin endocytosis in renal cells, which has broad prospects in exploring renal recapture function and screening kidney injury-related drugs.

Finally, we strived to explore the potential pocket by computational tools (Fig. S14 in Supporting information). According to the results of early virtual screening (Table S7 in Supporting information), in the top 10 poses, the preferred binding site was located at subdomain IB, distinct from two major drug sites. The predicted binding site had an 80% chance of being occupied by **7-HTCF**. Beside, two online tools, PARS and CavityPlus, found eight (Table S8 in Supporting information) and ten possible pockets (Table S9 in Supporting information), respectively, with these predicted sites located at or near IB. All the possible outcomes consistently point to IB. Therefore, the pose in the subdomain IB was targeted for dynamics simulation under near-physiological conditions. Molecular dynamics (Fig. 6A) further suggested that such binding mode was exceedingly stable with an RMSD value of less than 0.3. The binding free energy of **7-HTCF** towards HSA was −137.1 kJ/mol. By comparison, the binding of AAG to the probe was less sturdy with a binding free energy of −61.4 kJ/mol (Fig. S15 in Supporting information). In the best-predicted pose (Fig. 6B and Fig. S16 in Supporting information), the aromatic center of coumarin interacted with TYR138 and TYR161 to generate π-π stacked and π-π T-shaped interactions. Beside, **7-HTCF** was in contact with multiple residues by van der Waals interactions and pi-alkyl hydrophobic interactions. These results were highly consistent with the previous outcomes.

In summary, inspired by the powerful ligand-binding ability of HSA, a novel TICT-based NIR sensor (**7-HTCF**) was developed for light-up sensing and imaging HSA in human plasma and living cells. Under physiological conditions, **7-HTCF** could tightly bind HSA at a non-drug binding site to form a stable complex, with a 1:1 stoichiometry. The **7-HTCF**-HSA complex could emit strong fluorescence signals around 670 nm, accompanied by remarkable changes in both color and fluorescence emission. **7-HTCF** based fluorescence assay has been well-characterized and the results demonstrate that **7-HTCF** displays a good combination of the fluorescence response, high sensitivity, excellent chemical and photochemical stability, and outstanding selectivity towards HSA. With the help of **7-HTCF**, the levels of HSA in diluted human plasma can be precisely quantified, while the reabsorbed HSA in living renal cells can be *in-situ* monitored visually. Collectively, this study offers a practical optical sensor for highly selective sensing HSA in a variety of biological systems including plasma samples and living cells, which provides a promising tool for investigating HSA-associated biological processes and for clinical diagnosis of human diseases.

Declaration of competing interest

The authors declare that they have no known competing financial interests or personal relationships that could have appeared to influence the work reported in this paper.

Acknowledgments

This work was financially supported by the National Key Research and Development Program of China (No. 2021YFE0200900), National Natural Science Foundation of China (Nos. 81922070, 81973286, 82003847, 81703604), Shanghai Science and Technology Innovation Action Plans (Nos. 20S21901500 and 20S21900900) supported by Shanghai Science and Technology Committee, Innovation Team and Talents Cultivation Program of National Administration of Traditional Chinese Medicine (No. ZYYCXTD-D-202004), Shanghai Talent Development Fund (No. 2019093), and Shanghai University of Traditional Chinese Medicine Postgraduate Innovation Training Special (No. Y2021034).

Supplementary materials

Supplementary material associated with this article can be found, in the online version, at doi:10.1016/j.cclet.2022.05.071.

References

[1] G.J. Quinlan, G.S. Martin, T.W. Evans, Hepatology 41 (2005) 1211–1219.
[2] Q. Jin, L. Feng, S.J. Zhang, et al., Anal. Chem. 89 (2017) 9884–9891.
[3] V. Arroyo, R. Garcia-Martinez, X. Salvatella, J. Hepatol. 61 (2014) 396–407.
[4] G. Fanali, A. di Masi, V. Trezza, et al., Mol. Asp. Med. 33 (2012) 209–290.
[5] Z. Liu, X. Chen, Chem. Soc. Rev. 45 (2016) 1432–1456.
[6] S. Sen, R. Williams, R. Jalan, Am. J. Gastroenterol. 100 (2005) 468–475.
[7] E. Moujaess, M. Fakhoury, T. Assi, et al., Crit. Rev. Oncol. Hematol. 120 (2017) 203–209.
[8] R. Spinella, R. Sawhney, R. Jalan, Hepatol. Int. 10 (2016) 124–132.
[9] K. Oettl, R. Birner-Gruenberger, W. Spindelboeck, et al., J. Hepatol. 59 (2013) 978–983.
[10] J.F. Xu, Y.S. Yang, A.Q. Jiang, et al., Crit. Rev. Anal. Chem. 52 (2020) 72–92.
[11] A. Jahanban-Esfahlan, L. Roufegarinejad, R. Jahanban-Esfahlan, et al., Talanta 207 (2020) 120317.
[12] D. Kumar, D. Banerjee, Clin. Chim. Acta 469 (2017) 150–160.
[13] W. Li, D. Chen, H. Wang, et al., ACS Appl. Mater. Interfaces 7 (2015) 26094–26100.
[14] Y. Xu, M. Zhang, B. Li, et al., Talanta 185 (2018) 568–572.
[15] S. Aitekenov, A. Gaipov, R. Bukasov, Talanta 223 (2021) 121718.
[16] G. Rabbani, S.N. Ahn, Int. J. Biol. Macromol. 123 (2019) 979–990.
[17] P. Xing, Y. Niu, R. Mu, et al., Nat. Commun. 11 (2020) 1573.
[18] S. Delanghe, W.V. Biesen, N.V. Velde, et al., Clin. Chem. Lab. Med. 56 (2018) 436–440.
[19] M.B. Kok, F.P. Tegelaers, B. van Dam, et al., Clin. Chim. Acta 434 (2014) 6–10.
[20] Y. Kim, E. Shin, W. Jung, et al., Sensors (Basel, Switzerland) 20 (2020) 1232.
[21] M. Zhao, B. Li, H. Zhang, et al., Chem. Sci. 12 (2020) 3448–3459.
[22] F. Yan, J. Cui, C. Wang, et al., Chin. Chem. Lett. 33 (2022) 4219–4222.
[23] Q. Jin, H. Ma, L. Feng, et al., Chin. Chem. Lett. 31 (2020) 2945–2949.
[24] S. Lee, D.B. Sung, S. Kang, et al., Sensors (Basel, Switzerland) 19 (2019) 5298.
[25] N. Kishikawa, K. Ohyama, A. Saiki, et al., Anal. Chim. Acta 780 (2013) 1–6.
[26] G. Bassolino, C. Nancoz, Z. Thiel, et al., Chem. Sci. 9 (2018) 387–391.
[27] H. Fujioka, S.N. Uno, M. Kamiya, et al., Chem. Commun. 56 (2020) 5617–5620 (Camb).
[28] C. Wang, W. Chi, Q. Qiao, et al., Chem. Soc. Rev. 50 (2021) 12656–12678.
[29] S. Samanta, S. Halder, G. Das, Anal. Chem. 90 (2018) 7561–7568.
[30] S.I. Reja, I.A. Khan, V. Bhalla, et al., Chem. Commun. 52 (2016) 1182–1185 (Camb).
[31] Y.R. Wang, L. Feng, L. Xu, et al., Chem. Commun. 52 (2016) 6064–6067.
[32] A. Abbotto, L. Beverina, N. Manfredi, et al., Chemistry 15 (2009) 6175–6185.
[33] X. Liu, J.M. Cole, Z. Xu, J. Phys. Chem. C 121 (2017) 13274–13279.
[34] P. Zhang, X. Guo, Y. Xiao, et al., Spectrochim. Acta A Mol. Biomol. Spectrosc. 223 (2019) 117318.
[35] Y. Chen, J. Liu, M. Song, et al., Spectrochim. Acta A: Mol. Biomol. Spectrosc. 203 (2018) 158–165.
[36] M.P. Czub, K.B. Handing, B.S. Venkataramany, et al., J. Med. Chem. 63 (2020) 6847–6862.
[37] F. Yang, Y. Zhang, H. Liang, Int. J. Mol. Sci. 15 (2014) 3580–3595.
[38] J.Y. Guh, Nephrology (Carlton) 2 (15 Suppl.) (2010) 53–56.
[39] A.S. De Vriese, D.L. Robbrecht, R.C. Vanholder, et al., Am. J. Kidney Dis. 31 (1998) 108–115.
[40] J.S. Kim, K.J. Kim, E.Y. Choi, Medicine (Baltimore) 97 (2018) e10556.